University of Nairobi

Institute of Nuclear Science & Technology

ENVIRONMENTAL RADIATION MONITORING USING THERMOLUMINESCENCE DOSIMETRY IN KWAVONZA AREA, KITUI COUNTY

By

EVALYNE JEMUTAI CHERUIYOT

S56/70446/2011

A thesis submitted in partial fulfilment for the degree of Master of Science in Nuclear Science of the University of Nairobi.

Declaration

This thesis is my original work and has not been presented for a degree in any other university

Signature _____

Date_____

Approval

This thesis has been submitted for examination with our approval as university supervisors.

Mr. David Maina
Institute of Nuclear Science and Technology,
University of Nairobi

Signature _____ Date _____

Prof. Michael Gatari,
Institute of Nuclear Science and Technology,
University of Nairobi

Signature_____ Date _____

Dedication

I dedicate this work first and foremost to God in who is the key to all my success and to my family.

Acknowledgement

I am greatly thankful to God for enabling me to begin and end this work successfully. To my lead supervisor Mr. David Maina, i say may God reward you beyond all measures for your efforts in making this work a success. My gratitude goes to my second supervisor Prof. Michael Gatari, for your support and guidance throughout the period of this work. I also acknowledge the inputs of the Kenya Radiation Protection Board and especially Mr. Arthur Koteng, Mr. Joseph Maina and Mr.Erustus Chepkwony for your advice and contribution. I also thank the staff of South Eastern Kenya University (SEKU) who contributed a lot during my fieldwork. I am also indebted to my family, for their moral, spiritual and financial support besides their care, love, support and understanding and may God's blessings be upon you always. Finally, I thank all my friends whose contribution to this work made it a success, may God reward you all.

Abstract

Exposure to ionizing radiation can cause health hazards. The annual effective dose from both natural and man-made radiation sources globally is about 3 mSv. Of this dose, 80% (2.4 mSv) comes from natural background radiation, although these levels vary greatly from place to place. Mineral rich areas usually experience high levels of environmental radiation because radionuclides that occur alongside these minerals deep underground are exposed to the surface during the process of mining.

The objective of this study was to determine environmental gamma radiation levels in Kwa-Vonza area, Kitui County. This is because Kitui County is a mineral rich region that has been mapped for future mining operations which may result in exposure to high levels of ionizing radiation thereby causing radiation related health hazards. Thermoluminescence technique together with a NaI(Ti) based survey meter were used to measure the exposure levels. Thermoluminescence dosimeters made of CaF_2: Dy (TLD- 200) were prepared and deployed to the study area for a period of one month. They were then withdrawn and read using a Thermoluminescence card reader to determine the dose and dose rates. The results ranged between 4 - 63 nGy h^{-1} while the average absorbed dose was 29.33 ± 15.86 nGy h^{-1}. This gave an annual effective dose equivalent of 0.188 ± 0.019 mSv y^{-1} which is much lower than the 1 mSv y^{-1} maximum allowed occupational dose set by the ICRP.

Table of contents

List of Abbreviations

UNCEAR- United Nations Scientific Committee on the Effects of Atomic Radiation

TLD- Thermoluminescence Dosimeter

TL-Thermoluminescence

EMBS-Eastern Mozambique Belt Segment

TTP- Time Temperature Profile

List of tables

List of figures

CHAPTER 1

INTRODUCTION

1.1 Background

Ionizing radiation describes all forms of radiation with enough energy to strip electrons from atoms, thus creating charged or ionized atoms. They include X-rays, gamma rays, alpha particles, beta particles, sub-atomic particles, heavy charged particles and neutrons. Ionizing radiation is dangerous because it causes ionization in atoms of living cells which causes cell death or cell mutations that can lead to cells becoming cancerous.

Ionizing radiation originates from both natural and artificial sources. The natural sources include high-energy cosmic ray particles, radionuclides found in the earth's crust and those that exist within the human body. Man-made or artificial sources include X-rays, radionuclides used in medical procedures, manufactured products, nuclear fallout and nuclear waste. In addition, human activities like mining often lead to the concentration of the natural sources in the environment. This happens when earth crust products like minerals, coal and oil are being extracted, refined and used.

The detection and measurement of the amount of ionizing radiation present is important in order to identify the sources and take the necessary measures to avoid or reduce exposure. The amount of ionizing radiation released by a material is known as radioactivity and its units of measure are Becquerel (Bq). Exposure is the amount of radiation that is travelling through air and its units of measurement are coulombs per kilogram (C/Kg). The absorbed dose describes the quantity of energy that is placed by radioactive sources in an object or a person that they pass through. The units for absorbed dose is Gray (Gy) but when the medical effects associated with absorbed dose

in considered, it is known as the effective dose which has Sieverts (Sv) as the unit of measurement.

According to UNSCEAR (2008), the worldwide average natural radiation dose from cosmic, terrestrial and internal radiation sources is 2.4 mSv yr^{-1}, which is four times the worldwide average man-made radiation dose of 0.6 mSv yr^{-1}. Cosmic radiation originates from the outer space and mainly consists of protons. The worldwide average radiation dose at sea level due to cosmic rays is 0.39 mSv yr^{-1}.Terrestial radiation comes from natural radionuclide sources in the earth's crust which include primordial ^{40}K and decay products of uranium (^{238}U and ^{235}U) and ^{232}Th. UNSCEAR (2008) further gives the average worldwide dose due to terrestrial sources as 0.48 mSv yr^{-1} and an average worldwide dose of 0.29 mSv yr^{-1} and 1.26 mSv yr^{-1} from food and inhaled radon respectively. The internal exposure is mainly from naturally occurring ^{40}K within the human body together with ^{222}Rn which is also considered as an internal source of ionizing radiation when inhaled.

According to UNSCEAR (2000), radioactive elements are not uniformly in the environment and their exposure varies by a factor of three worldwide. This is the reason for the varying levels of terrestial background radiation from one place to another. For example, there are regions in the world where the outdoor terrestrial radiation exceeds substantially the average value due to the enrichment of certain radioactive minerals leading to the formation of high background radiation areas. The presence of high background areas has been reported in several places: Ramsar in Iran with a maximum of 260 $mSvyr^{-1}$ (Ghiassi-nejad *et al.,* 2002), Guarapari in Brazil with 35$mSvyr^{-1}$(Pfeiffer *et al.,* 1981), Kuranagappaly in India with 35 $mSvyr^{-1}$ (Nair *et al.,* 1999) and Yangjiang in China with 5.4 $mSvyr^{-1}$ (Zha *et al.,* 1996) as seen in figure 1.1. High background

radiation areas in Kenya include areas along the Kenyan coast including Mrima hills (Mustapha *et al*., 2004), Homa Bay (Mustapha *et al.,* 1999) and Lambwe valley (Achola *et al*., 2012)

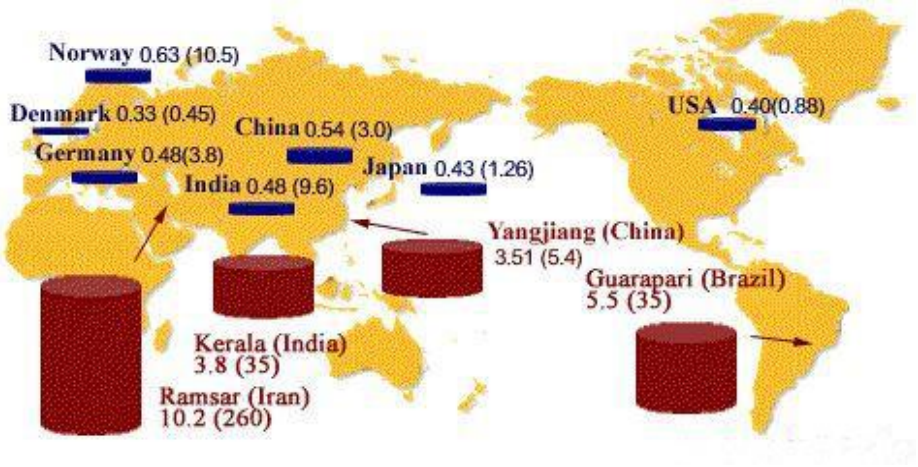

Figure 1.1: Doses for high background radiation areas around the world (mSv y^{-1}). The figures in brackets indicate the maximum value (Ghiassi-Nejad et al, 2002)

According to UNSCEAR (1993), background radiation contributed by cosmic sources varies from place to place depending on the latitude, altitude, and the solar magnetic activity cycle. The dose due to cosmic rays increases with altitude due to the decreasing depth of atmospheric layer which normally provide a shielding effect from cosmic radiation. For instance, the effective dose rate contributed by cosmic rays at sea level around the world is around 0.06 μSv h^{-1} but it increases to about twice at elevations of 1.6 km. Denver in the USA, nicknamed Mile-High City, has an altitude of 1.61 km and receives a dose rate of about 0.1 μSv h^{-1} while Mexico City with an altitude of 2.25 km receives 0.2 μSv h^{-1}. Places with higher altitudes like Lhasa, Tibet (3.7 km) and the peaks of the Himalayas Mountains (6.4 - 8 km) have dose rates reaching 1 μSv h^{-1}. Those travelling by plane at altitudes of 10 km and 15 km receive doses of up to 5μSv h^{-1} and 10 μSv h^{-1} respectively (Dyer *et al.,* 2007). The variation of cosmic rays due to latitude and solar

cycle is by a factor of two whereby the dose is less at the equator than at the poles which is attributed to the effects of the earth's magnetic field (magnetosphere). This field deflects charged cosmic ray particles like carbon-14, tritium and beryllium-7 maximally at the equator and minimally at the poles leading to high cosmic radiation at the poles (Enyinna, 2016).

All human beings are always exposed to background radiation. This is because their exposures are impossible to control in particular areas that have significantly high levels that present high health risks. Human activities, such as mining, enhance the levels of background radiation by producing large amounts of naturally occurring radioactive material (NORM) and depositing them to the surface of the earth which would have otherwise been buried deep underground. The levels of such technologically enhanced naturally occurring radioactive materials (TENORM) should therefore be controlled by regulatory bodies.

1.2 Radioactivity and mining

In Kenya, a wide variety of minerals are known and mapped, but a great potential lies in the recently discovered mineral deposits. Indeed, the discovery of over 200 million tonnes of coal in Kitui County, about 750 million barrels of oil in Turkana County and substantial amounts of heavy mineral sands along the country's south-eastern coast will shape the entire mining industry which has been largely influenced by the production of non-metals such as soda ash, limestone, kaolin, fluorspar, and gemstones. Kitui region is also endowed with substantial quantities of other minerals including limestone, iron ore, copper, gypsum and sand among others.

In almost every mining region, uncontrolled mining has caused degradation of land, topographical disorders, ecological imbalances and disrupted land use patterns in a majority mining regions around the world (Ghose, 1989).The sand harvesting business in the entire

eastern region of Kenya is booming due to the ever growing demand in the construction industry mainly in the Nairobi city and its environs. As a result, sand harvesters have invaded the seasonal rivers in search of the commodity. Like other sand harvesting areas in the country, the main environmental concern is usually the huge holes left after sand harvesting and the consequent diversion of rivers. However, other effects associated with sand harvesting are yet to be dealt with. For example, the presence of traces of natural radionuclides incorporated in heavy minerals found in sand elevates the levels of environmental radioactivity which may pose health risks to the sand harvesters and the public in general.

Figure 1.2 Black sand deposits along RiverTiva in Kwa-Vonza, Kitui County

Black sands are used by prospectors to indicate the presence of placer formations. This is because black sand concentrates usually contain heavy minerals like ilmenite, monazite, tungsten, zirconium and rare earth bearing minerals. These radionuclide bearing minerals occur with sand deposits as sand grains mixed in with lighter clays and quartz. They are usually eroded from the surrounding bedrock and concentrated in the river channels and beaches due to the specific gravity of the mineral grains (2.9 g/cm^3). Monazite, for example, is a highly insoluble rare earth mineral that occurs in sand while ilmenite is titanium bearing mineral containing

oxides of titanium and iron also incorporated in sand. Black sand beaches containing these minerals are responsible for the world's highest background radiation areas of Brazil, India and China (Eisenbud *et al.*, 1997).

1.3 The Uranium and Thorium decay chain

The major contribution of dose from natural background radiation is inhalation of radon. Radon is produced by the Uranium and Thorium decay chains as follows:

Uranium decay chain

$^{238}U \longrightarrow {}^{234}Th \longrightarrow {}^{234}Pa \longrightarrow {}^{234}U \longrightarrow {}^{230}Th \longrightarrow {}^{226}Ra \longrightarrow {}^{222}Rn \longrightarrow {}^{218}Po \longrightarrow$

$^{214}Pb \longrightarrow {}^{214}Bi \longrightarrow {}^{214}Po \longrightarrow {}^{210}Pb \longrightarrow {}^{210}Bi \longrightarrow {}^{210}Po \longrightarrow {}^{206}Pb$ (stable)

Thorium decay chain

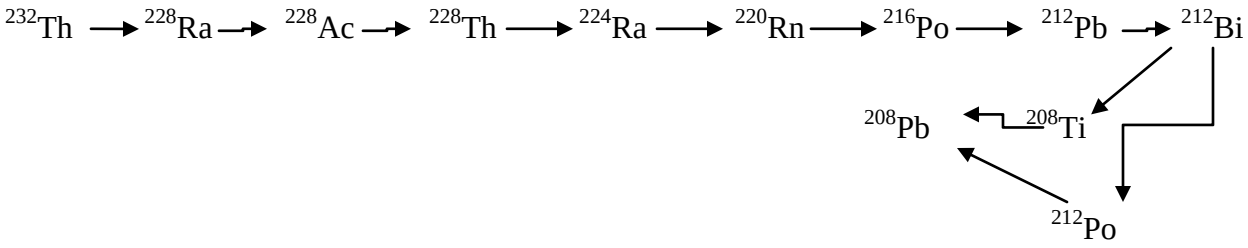

($\longrightarrow$ Alpha decay, $\longrightarrow$ Beta decay)

The alpha decay of ^{226}Ra and ^{224}Ra found in natural soils, rocks and mineral ores produce radionuclide noble gases ^{222}Rn and ^{220}Rn respectively. Radon is an inert gas and it diffuses through the soil into the atmosphere whereby its exposure is associated with various cancers. This is especially so if uranium rich compound lie close to the earth surface (UNSCEAR, 1993). The decay products of radon like Bi, Pb, and Po also get attached to aerosols to become part of

the particulate matter in the air. When this happens, they can only get removed through radioactive decay, surface deposition or washout by rain.

Ionizing radiation can cause genetic changes in cells that alter their ability to regulate the rate at which they reproduce leading to the growth of cancers like leukemia, melanomas as well as kidney and prostate cancers. Forster (2002), reports an increased number of mutations in the DNA of the people living in the high natural background radiation area of Kerela, India whereby there were 22 mutations in their mitochondrial DNA sequences compared to only one mutation in those living in low-radiation area. Zakeri *et al.* (2011) also noted a significant increase in the occurrence of abnormalities detected in unstable chromosomal aberrations which was attributed to elevated background radiation levels in Ramsar, Iran. Masoomi *et al.* (2006) found a higher level of spontaneous DNA damage in blood samples of people living in HNBR areas of Ramsar. However, other studies like Hendry *et al.* (2009) and Mortazavi *et al.* (2005)) did not report any detrimental biological effects in residents of high background radiation areas. Interestingly, Cohen (1995), Mortazavi *et al.* (2005), and Thomson (2011) report a negative relation between radon concentrations and the number of occurrences of lung cancer.

1.4 Environmental Radiation Monitoring

Although people have always been unsheltered from different kinds of radiation since the creation of life on earth, it was not until the last century that mankind became aware of all these radiations that come from space, soil, sea, air and even their own body. Today, ionizing radiation and radioactive materials are highly used in the fields of medicine, industry and research which in turn have led to enhanced levels of harmful radiation in the environment. These radiations are highly dangerous, since they are not sensed by any of the five sensors of human body. Luckily,

techniques have been developed for assessing these radiation exposures from the environment on the general public to guarantee their safety.

The distribution of terrestrial radiation highly varies depending on the geology of the earth but, human activities have enhanced doses received from terrestrial radionuclides. These sources are of particular interest because they can be controlled, allowing for the management of exposures to radiation through regulated practice. Such sources include mining operations, nuclear waste disposal, emissions from nuclear power, nuclear weapons, reprocessing plants and so on.

Environmental radiation monitoring focuses on the impact of environmental radiation on the general public. Watchdog pressure from the community, health sector, environmentalists and the political class, has led to continuous environmental radiation monitoring becoming a requirement in many countries especially in areas that are close to manmade sources. Man-made radiation sources represent less than 0.1% of the entire environmental dose while natural radiation sources account for the remaining 99.9% (UNSCEAR, 2008). This is why it is necessary to establish the doses as a result of natural background radiation.

Since a large percentage of the annual radiation dose to individuals is as a result of external radiation from natural radionuclides in the environment (UNSCEAR, 2000), radiation detectors such as thermoluminescence detectors have been used in environmental radiation monitoring because they allow for the measurements of long-term accumulation of doses distributed in the environment of radioactive materials around the world. They are sensitive, durable, simple, accurate and stable allowing for short and long term radiation monitoring despite the occurrences of adverse weather.

1.5 Environmental radiation doses and dose limits

The average radiation absorbed dose due to background radiation has been measured in many countries of the world. Among the highest figures were those of Hong Kong (1.41 mSv y^{-1}), Australia (0.81 mSv y^{-1}), Portugal (0.73 mSv y^{-1}) and Romania (0.7 mSv y^{-1}). The lowest dose rates have been registered in Canada (0.2 mSv y^{-1}), Iceland (0.25 mSv y^{-1}), United Kingdom (0.31 mSv y^{-1}) and the Netherlands (0.29 mSv y^{-1}). In Africa, the highest dose rates have been recorded in Namibia (1.05 mSv y^{-1}) and the lowest in Egypt (0.28 mSv y^{-1}), (UNCEAR, 2000). In these measurements, the dose received indoors was higher than the ones received outdoors which is attributed to radionuclides present in building materials (Hendry *et al*., 2005).

In Kenya, various studies on radioactivity levels in the environment have been done. Mustapha *et al.,* (1999) carried out a study to assess human exposures to natural radiation in Nairobi, Kiambu, Kwale, Mombasa, Machakos, Bungoma and Transzoia areas. They reported an average effective dose of 3.79 mSv y^{-1} which was slightly above the world average of 2.4 mSv y^{-1}. Other studies which have been carried out include Maina *et al.,* (2002) on indoor radon levels in Coastal and Rift Valley regions and Agola (2006) on natural radiation levels in Olkaria Geothermal region among other studies.

The ICRP philosophy on dose limits to the public, which is followed by many countries, recommends an effective dose limit to the general public of 1 mSv y^{-1}. Under special circumstances, it recommends that a higher dose be accepted given that the average over 5 years does not exceed 1 mSv y^{-1} (NCRP, 1991). However, these dose limits are used to regulate man-made radiation sources and not situations involving natural background radiation which are

impossible to regulate. The debate on whether such levels actually lead to harmful health effects or the linear no threshold model is adequate is still on.

1.6 Research problem

Kitui County is now considered a mineral rich region. These minerals sometimes occur together with heavy minerals that usually contain radionuclides. The establishment of these mining and processing operations may lead to increased levels of environmental radioactivity due to traces of radionuclides associated with the ores which pose potential radiation risks. It is, therefore, important to obtain data which will not only form a basis for radiation protection guidelines but also help in establishing preoperational external radiation levels for these new facilities for future monitoring purposes.

The local population may be exposed to radiation through several sources. First is through radiation from internal doses through food intake which includes alpha and beta emitting radionuclides that are present in plants and animals. Second is through the airborne particulate matter that may contain inhalable particles like monazite and/or thorium containing alpha emitting parent radionuclides and their associated daughter products. Third, is through the external doses of gamma radiation from soils and rocks containing gamma active nuclides as well as the alpha emitting gases thoron and radon. Despite being a mineral rich region, previous studies (Sanders, 1954; Dodson, 1953) were mainly geological and did not include natural radioactivity levels in the region.

1.7 Objectives.

1.7:1 Main objective

The main objective is to determine the environmental background radiation levels in Kwa-Vonza area, Kitui County. (Dodson, 1953)

1.7:2 Specific objectives

The specific objectives are:

- To determine the accumulated outdoor doses at background levels in air, 1 meter above the ground using TLDs.
- To compare the results obtained with those from similar studies in other parts of the world.

1.8 Justification.

Determination of background radiation levels is not only important in evaluation of radiological health impacts but also act as biological and geological chemical tracers in the environment. The data obtained will be of importance to the Radiation Protection Board, which is responsible for radioactivity mapping, monitoring and protection in the country. The radioactivity data from such regions will help in designing radiation protection control guidelines.

The society need to be educated on the benefits, opportunities and effects of the mining activities. For this to be achieved, this study will act as a basis for estimating environmental radiation doses and gauging the repercussions of radioactive pollution for the health of the people and the environment in the region as a result of future mining operations.

CHAPTER 2

LITERATURE REVIEW

This chapter describes some of the studies that have been carried out for the measurements of environmental radioactivity at different environments of the world using various radiation detection instruments. The biological effects of radiation, weighting factors as well as the instrumentation of the study are also described.

2.1 Radioactivity studies carried out in different parts of the world

Environmental radioactivity studies have been done in various parts of the world. Many of them have been carried out to determine the levels of natural radionuclides in soils from which the estimations of the absorbed dose were made. There have also been studies to determine the levels of radon and its exhalation rates given that radon contributes the largest percentage of natural radioactivity and radiological hazards in the environment. Other studies focused on direct measurements of environmental radiation in situ and the results integrated over certain periods of time.

Oktay *et al*. (2011) accessed the natural radioactivity and radiological hazards in building materials in Elazig, Turkey. They reported the specific concentrations that ranged from 3.5-114.1 Bq kg^{-1}(^{238}U), 1.6-20.7 Bq kg^{-1} (^{232}Th) and 201.4-4928.0 Bq kg^{-1} (^{40}K). The calculated radium equivalent value was 36.5Bq kg^{-1} in bricks and 405.2Bq kg^{-1} in gas concrete with average indoor radon concentrations of 364.3 Bq m^{-3}.

Al Mugren (2015) assessed the natural radioactivity levels and radiation dose rates in soil samples from Al-Rakkah, a historical site in Saudi Arabia. He found the mean activity

concentration in surface soils to be 23 ± 1.6 Bqkg^{-1}, 20 ± 1.4 Bqkg^{-1} and 233 ± 12 Bqkg^{-1}for ^{226}Ra, ^{232}Th and ^{40}K respectively. The total absorbed dose rate ranged between 17.74 - 72.24 nGyh^{-1} which provided a mean of 32.69 nGyh^{-1} which yielded an annual effective dose of 0.37 mSvy^{-1}.

Karunakara *et al*., (2014) assessed the gamma dose rates within a possible uranium mining site in southern India whereby direct and integrated measurements together with soil sample analysis for ^{226} Ra, ^{232}Th and ^{40}K activity were done. The geometric mean value of outdoor and indoor gamma dose rates were found to be 97 nGy h^{-1}and 104 nGy h^{-1}respectively. They also did a correlation study which exhibited a better correlation of the estimated dose from soil radioactivity measurements with direct measurements by the survey meter compared to the TLD measurements. They therefore concluded that the measurements by the survey meter give a better representation of gamma dose rates especially in a region having localized mineralization.

Santawamaitre (2012) evaluated the levels of NORM in soil samples along Chao Phraya river basin, Thailand. He found the activity concentrations for ^{238}U, ^{232}Th and ^{40}K to be 13.9-76.8, 12.9- 142.9 and 178.4- 810.7 Bq kg^{-1} respectively. He estimated the absorbed gamma dose rate in air at 1 meter above the ground to be in the range of 21.7 - 155.7 nGy h^{-1} which gave an annual effective dose equivalent range of 26.6- 190.9 µSv y^{-1} and an arithmetic mean value of 79.06 µSv y^{-1}. These activity concentration values for ^{238}U, ^{232}Th and ^{40}K were comparable to the world average values of 35, 30 and 400 Bq kg^{-1} respectively as well as the respective worldwide effective dose of 70 µSv y^{-1} (UNCEAR, 2000).

Bavarnegin *et al*., (2012) studied the radionuclide concentration in Ramsar, northern Iran and found the average values of 16 ± 6, 25 ± 11, and 280 ± 101 Bq kg^{-1} for ^{226}Ra, ^{232}Th, and ^{40}K levels respectively.

In West Africa Masok *et al*., (2015) assessed the outdoor and indoor background radiation levels in Plateau State University, Nigeria. They found a mean equivalent dose rate for outdoor background radiation to be 0.249 μSv h^{-1} and indoor background radiation to be 0.256 μSv h^{-1}. The computed mean annual equivalent dose rate for outdoor and indoor background radiation level was found to be 0.44 mSv y^{-1} and 1.54 mSv y^{-1} respectively. The values obtained were below the world average dose of 2.4 mSv y^{-1}. Also, Ajayi *et a.l* (2009) studied the radioactivity of some sachet drinking water produced in Nigeria and found activity concentration values that ranged from 0.57 - 34.08 Bq L^{-1}, 2.22 - 15.50 Bq L^{-1} and 0.04 - 7.04 Bq L^{-1}. These values gave an estimated annual effective dose of 4.73 - 49.13, 1.21 - 12.26, 0.86 - 8.54, 1.22 - 11.66, 3.40 - 28.98 and 0.68 - 5.04 mSv y^{-1} for different age groups. Jibiri *et al*., (2011) studied terrestial gamma dose rates in former tin mining area in Jos-Plateau and found the radionuclide activity concentration in farm soils to be higher than the world average figures for normal background radiation.

Sroor *et al.,* (2011) studied the radioactivity levels and exhalation rate of ^{222}Rn of soils in southern parts of Egypt. 30 soil samples from mining sites were taken and analyzed for radio nuclides concentrations and the measurements of ^{222}Rn concentration and exhalation rates from the samples were also done. The radon concentration values varied from 1.54 - 5.37 $BqKg^{-1}$ while exhalation rates ranged between 338.81 - 1426.47 Bqm^{-2} d^{-1}. They concluded that the knowledge of uranium concentrations is enough to give the estimation of ^{222}Rn in the soil as well as its escape into the atmosphere.

Abiama *et al*., (2010) investigated background radiation in three areas of southwestern Cameroon. They found a mean activity concentration of 0.13 ± 0.01 kBq kg^{-1} for ^{226}Ra,

0.39 ± 0.03 kBq kg^{-1} for ^{232}Th and 0.85 ± 0.07 kBq kg^{-1} for ^{40}K. This gave an estimated outdoor mean annual effective dose of 0.48, 0.39 and 0.38 mSv y^{-1} in the three study areas.

In East Africa, Mohammed *et al.*, (2013) studied the radioactivity in soil and water samples from around Mkuju uranium deposit, Tanzania. They obtained concentrations in soil samples on average to be 51.7 Bq kg^{-1} (^{238}U), 36.4 Bq kg^{-1} (^{232}Th), and 564.3 Bq kg^{-1} (^{40}K). They also found the average radioactivity concentration values in water samples to be 2.35 BqL^{-1} (^{238}U) and 1.85 BqL^{-1} (^{232}Th). Masore *et al*., (2007) also studied the natural radioactivity levels in surface soils around the then proposed titanium mining site in Kwale district, Kenya. They reported the radioactivity concentration ranges and mean of 8.4 - 43.6 (27.6) Bq Kg^{-1} for ^{232}Th, 7.4 - 40.6 (20.9) Bq Kg^{-1} for ^{226}Ra and 31.9 - 114.1 (69.5) Bq Kg^{-1} for ^{40}K. The calculated mean absorbed dose rate in air from the radioactivity concentrations was found to be 25.2 nGy h^{-1}, which is equal to an effective dose rate of 62.0 uSv y^{-1}.

Mulwa *et al.,* (2013) performed a study on the radiological analysis of suitability of Kitui south limestone for use as building material. This study was carried out in the areas Kituvwi, Mwanyani and Ndulukuni in Kitui South and obtained the gamma activity index that ranged from 0.13 to 0.21 which showed that the limestone samples could be used without the risk of elevated indoor exposure.

2.2 Biological effects of radiation

The discovery of ionizing radiation by Wilhelm Roentgen in 1895 was a great breakthrough but it was not until shortly afterwards that its potentially deleterious health effects were identified. Patients who were administered x-rays started experiencing radiation burns on the skin and in the eyes. In 1915, a resolution on x-ray safety was adopted after it was discovered that radiation could both cause and treat cancer (Turner, 2008).

Radiation causes biological damage primarily by creating free radicals in cells which can cause alterations in DNA by breaking the sugar backbone of the DNA molecule or chemically altering the DNA bases. These, in turn, could both lead to changes in the DNA code when it is repaired or copied, leading to changes in the biological properties of the cells affected by radiation. Although DNA damage usually lead to individual cell repair or programmed cell death (apoptosis), others manage to live on with a mutation which can cause problems for the whole organism. This is especially the case whereby high radiation doses tend to increase cancer risk because the number of cells that do survive with mutations increase (Cember and Johnson, 2008.)

According to Trap and Kron (2008), the biological effects of radiation can be deterministic, stochastic, somatic or hereditary. Deterministic effects are those that occur above a certain threshold of radiation dose with the severity of the resulting injury increasing with the dose. They include radiation burns to the skin, temporary immune deficiency, and gastrointestinal tract damage. At the highest doses, people may lose consciousness in a matter of minutes and die relatively soon after exposure (Cember and Johnson, 2008)

Stochastic effects occur at all dose levels without any threshold value and the chance of injury occurring increases with the increasing dose. The severity of the injury is also not dependent on the dose that induced it. They include all the late expressing health effects of radiation like cancer except those that result from direct radiation (Matthews and Brennan, 2008)

Somatic effects appear after acute radiation exposure and include organ death, vomiting and nausea, cancer, cataracts and reduced life expectancy. Hereditary effects are those that occur in the offspring of an irradiated individual and the approximated risk of severe ill health within the initial two generations is 10 pm/mSv with the risk being double in subsequent generations (Martin & Harbison, 1996)

2.3 Weighting factors

Body tissues are different hence have different sensitivities to radiation. The biological effects of radiation are most strongly associated with cells that are dividing and as these cells move through the cell cycle, they must pass through several 'checkpoints' which are molecular mechanisms for verifying the integrity of the cell's DNA before it is copied. If the DNA is damaged, the cell either repairs the damage or it undergoes apoptosis. When the cell attempts to repair the DNA damage, it can occasionally do so through an error prone pathway that can lead to loss of DNA segments or changes in the DNA sequence.

Unlike the nerve cells that do not need to divide often, cells like those of bone marrow are highly dividing and are very sensitive radiation effects (Cember & Johnson, 2008).Due to varying levels of cell sensitivities to radiation, different tissues are given different weighting factors when considering the whole body dose from a radiation source. The International Commission on

Radiological Protection (ICRP) regulates the updates and recommends weighting factors for various tissues when calculating the whole body dose equivalent as presented in table 2.1.

Table 2.1: Tissue weighting factors (Wrixon, 2008)

Tissue	**Weighting Factor, W_F**	**Sum of W_T Values**
(a) Red- marrow, lung,colon, stomach	0.12	0.48
(b) Bladder, breast, liver, oesophagus, thyroid, remainder tissues	0.05	0.30
(c) Gonads	0.20	0.20
(d) Bone surface, skin	0.01	0.02
Total		**1.0**

Remainder tissues are: adrenals, heart, muscle, extra thoracic region, spleen, gall bladder, kidneys, prostate, mucosa, thymus, pancreas, lymphatic nodes, small intestine, uterus/cervix.

Besides the differential sensitivities of tissues to radiation, all types of radiation produce different relative biological effects. The absorbed dose (Gy) depends on the energy of the radiation and type of the absorbing object. So, even with the same intensity, a high energy beam produces lower absorbed dose than a low energy beam because a majority of the high energy beam photons manage to pass without absorption in comparison to the low energy beam (Ball *et al*, 2008).

The density of ionization caused by a given type of radiation affects its biological effects. More densely ionizing types of radiation transfer their energy in a relatively smaller volume such as α-particles when compared to γ-rays and have relatively greater biological effects. Therefore, the concept of equivalent dose which takes into account the type and energy of the ionization

radiation that is deposited in any tissue is used. Equivalent dose (Sv) is the product of the absorbed dose (Gy) and the respective radiation weighting factor. The recommended values when converting Gy to Sv are shown in table 2.2.

Table 2.2: Radiation weighting factors (ICRP, 2012)

Radiation Type Radiation	**Weighting Factor, W_F**
Photons (all energies)	1
Electrons and muons (all energies)	1
Protons other than recoil, energy >2 MeV	5
Alpha particles, fission fragments, heavy nuclei	20
Neutrons < 10 keV	5
10 -100 keV	10
100keV-2 MeV	20
2- 20 MeV	10
>20 M	5

Effective dose (Sv) or the product of the equivalent doses to each organ and the respective tissue weighting factor is considered to be the whole body radiation dose. The dose rate allows for the calculation of dose over a given period of time because it is a measure of how fast a radiation dose deposited on a medium.

2.4 Radiation dosimetry

Radiation dosimetry is the process of calculating and assessing the radiation dose that is received by the human body. Routine environmental dosimetry is the practice of measuring everyday doses received by those who work around radiation sources and the public at large. This is to

ensure that the doses that they receive are as low as reasonably achievable so that health risks that are associated with high levels of radiation are avoided. Radiation dosimetry is usually a continuous process hence it should not interfere with the people that live or work there, it should be relatively inexpensive, and because large areas may need to be monitored, it should be easy to process hundreds or even thousands of dosimeters per year while providing accurate measurements of dose across disparate dose levels (Cember and Johnson, 2008).

Radiation dosimeters are devices, instruments or systems that measure quantities or rates of ionizing radiation. Generally, the different dosimeters used in radiation dosimetry are pen-type dosimeters, film dosimeters, electronic detectors, Thermoluminescence dosimeters (TLDs), and optically stimulated luminescence. Each of these types of dosimeters has its benefits and drawbacks and each dosimeter has characteristics which make it a good choice in a given situation. Apart from the benefits, the selection of different technologies, especially between closely related technologies, may depend on cost, business relationships, investments in capital goods like dosimeter readers, and amount of training required for technicians to operate a program amongst others.

2.5Thermoluminescence dosimetry

Luminescence occurs in a number of materials: plasma screens, discharge lamps, LEDs, CRTs and X-ray intensifiers among many others. Mechanisms of luminescence include fluorescence, phosphorescence and persistent luminescence (thermoluminescence, electroluminescence, photoluminescence, chemiluminescence and so on).Fluorescence is the prompt emission of light after energy input (nano seconds to micro seconds) while phosphorescence is a delayed florescence (milli seconds). Both fluorescence and phosphorescence do not require an additional trigger to occur.

Thermoluminescence (TL) is the emission of light in the process of heating of a solid sample (semiconductor or insulator) that has been previously exposed to radiation. While the property of thermoluminescence was known, it was not until the early 1950s that Farrington Daniels suggested it as a method for radiation dosimetry (McKeever et al, 1995). The TL material usually absorbs energy when exposed to radiation which it stores until it is heated. The intensity of the light that is emitted as a function of temperature (or time) gives the thermoluminescence glow curve (fig.2.1). The glow peaks are a function of various energy traps (Furetta and Weng, 1998).

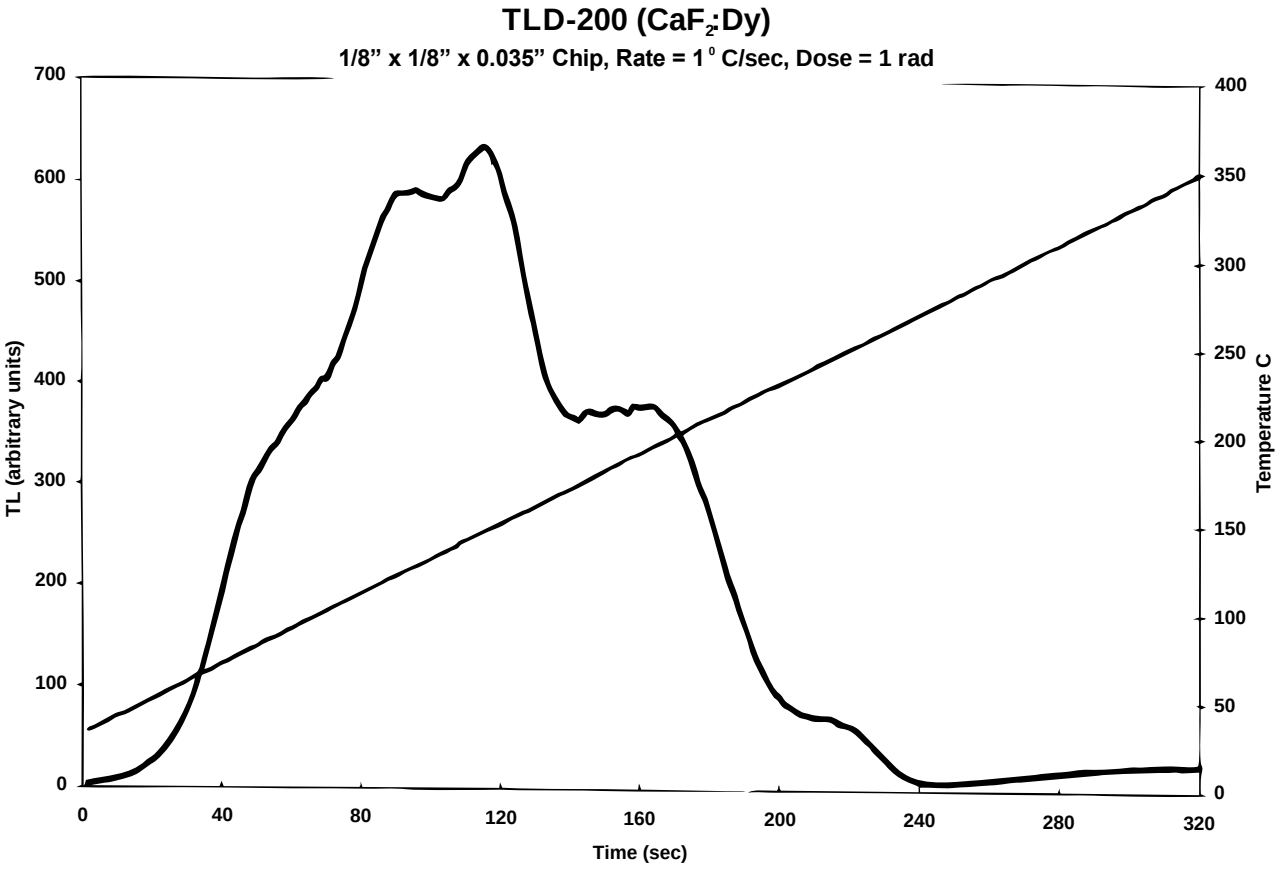

Fig 2.1 Example of a glow-curve (Furetta et al., 1998)

TL requires heating as a trigger and a TLD which has been irradiated but not heated will stay in a metastable state until such time as heating occurs. This is the principle behind one of the great

benefits of TLD – they can be worn without being read for weeks or months at a time before finally being read out without loss of dose information. When the TLD is heated, the emission of light is prompt and this is another beneficial feature because TLDs can be thought of as always being in one of two states: equilibrium and metastable states (McKeever *et al.*, 1995).

TLD materials are crystals with impurities and are usually enhanced by the addition of dopants at controlled amounts. Although the crystal structure is determined by the composition, dopants are usually present in relatively small amounts. These dopants create defects in the crystal structure which are important because they play a role in capturing the energy released in ionizing radiation interactions in the material (McKeever *et al.*, 1995). The role of lattice imperfections in semiconductors and luminescence is important because they determine the properties of the solid (Haug, 1972).

2.6. Principles of Thermoluminescence

The phenomenon behind thermoluminescence can be explained using the electron band theory which states that when a solid is exposed to radiation, electrons and holes are produced. In an ideal insulator at equilibrium, electrons reside in the valence band which is separated from the conduction band by a large gap known as forbidden gap. When sufficient energy is applied, electron scan jump to the conduction band through the forbidden gap between them. However, impurities cause the presence of localized energy levels (traps) within the forbidden gap because of defects in the solid. These are sites where electrons and holes can be trapped upon irradiation as shown in figure 2.2, where T represents the electron traps and L luminescence centers.

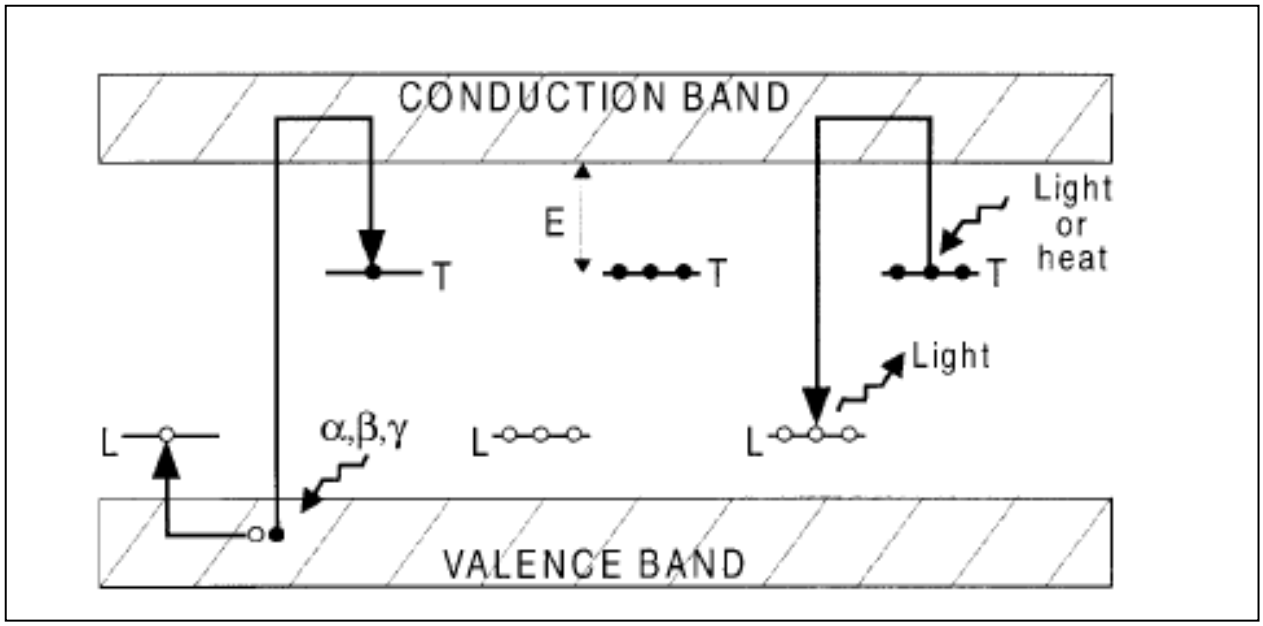

Figure 2.2.The energy level representation of a TL process

When the material is heated, the electrons and holes that are trapped receive enough energy to escape from the trap to the conduction or valence band where they recombine with trapped holes or electrons at the recombination centre. This is followed by emission of photons before the system goes back to the equilibrium state whereby a part of the excess energy is liberated as light. A complete thermoluminescence dosimetric system consists of the detector (TLD material), the TL reader and the measurement cycle.

2.7. Thermoluminescence dosimetric system

Thermoluminescence detectors are materials (natural and synthetic), that emit light whose intensity is proportional to the dose of irradiation(Stochioiu et al., 2004).The type of dosimetry material that is chosen is based on a number of characteristics: good sensitivity, low rate of fading, inexpensive to manufacture, good stability through multiple readout cycles and it should have a near-tissue equivalent effective Z. Tissue equivalence is though not important with

environmental dose estimation since the only interest is to get the quantity of absorbed dose (D) in Gray.

Although there is currently no ideal thermoluminescence dosimeter for all tasks, the most commonly used TL phosphors with decisive amount of dopants are lithium fluoride, lithium borate, calcium fluoride and calcium sulphate. The characteristics of calcium fluoride (CaF_2: Dy) detector is described in table 2.3:

Table 2.3. Characteristics of CaF_2: Dy (TLD 200)

Material Characteristic	**Value for CaF_2: Dy (TLD 200)**
Applications:	Environmental dosimetry
Forms:	powder, rods, chips, cards
Density:	3.18
Effective atomic number:	16.3
TL emission spectra range:	460nm, 484nm, 577nm (max=484nm)
Temperature of main glow peak:	180^oC
Sensitivity at ^{60}CO Rel. to LiF:	30
Energy response (30KeV/^{60}CO):	12.5
Useful range:	10uR-10^6R
Fading:	5% in 50 days with anneal
Anneal:	Pre-irradiation 500^oC @ 1hr
	Post-irradiation 100^oC for 20 minutes
Sensitivity to UV light:	High

Annealing is a thermal treatment of TL dosimeters, done in an oven or in a furnace. It consists of heating the TLDs to a specific temperature and keeping them at that temperature for a certain period of time before they are cooled down to room temperature at a certain rate. The annealing procedures can also be carried out in the reader if the dose received by the dosimeters is lower than 10 to 20mGy (Furetta, 2003). All detectors from a batch should be annealed identically in order to standardize the TL response. The importance of annealing is to empty all the traps. This means that the TL signal will be reset to zero.

A TLD reader has a planchet for placing and heating the TLDs, a photomultiplier tube (PMT) to detect and convert light into an electrical and an electrometer for recording the electrical signal from the PMT as a charge or current (Furetta and Weng, 1998).

In order to determine the evaluated dose value **De** from the TL readout value (TL response, M), a mathematical evaluation using the evaluation factor **Fe** is needed whereby:

$$\boldsymbol{De = Fe\ x\ M} \qquad \textbf{2.1}$$

The TL response can be represented either by the height of the peak or by the area under the TL curve. When the peak area method is used, the calibration factor **Fc** is as follows:

$$\boldsymbol{Fc = Dc/(M - Mo)} \qquad \textbf{2.2}$$

M is the mean TL signal of TLDs irradiated by a calibration dose **Dc** and **Mo** is the mean TL signal of unirradiated control detectors. **Fe** enables corrections to be made that become necessary due to background, individual sensitivity of the detectors, fading, non-linearity and energy dependence (Furetta and Weng, 1998

CHAPTER 3

METHODOLOGY

The general description of the study area, the materials that were used in the course of this work as well as the procedures that were followed in determining the effective dose in the area of study are given.

3.1 Study Area

Kitui County is a place in the southern part of Kenya having a altitude of between 1400 and 1800 meters above the sea level. Its topography consist of hilly ridges set apart by wide, low lying areas and to the eastern side is Yatta plateau. The climate is entirely arid and semi arid with rainfall being very erratic and unreliable usually accompanied by high rates of evaporation. There was recent discovery of coal and other minerals in the region, while other prospects for heavy minerals are ongoing. Most of the rivers in the area are seasonal and full of black sand. This means that during the rainy season there is a lot of deposition from all the surrounding areas mainly as sand which is harvested during the dry season. Sand harvesting therefore is one of the main economic activities in the region. The most prevalent diseases are malaria, respiratory infections, skin diseases and eye infections and the life expectancy is 57 years which is below the national average of 65 years (WHO). Geologically, Kitui County lies on the Eastern Mozambique Belt Segment (EMBS) of Kenya which is a continental transition zone between the Mozambique belt of the north and south in Eastern Africa (Sanders, 1954).

The study area was divided into 3 zones each within a shopping center about a radius of 20 kilometers from the main location which was Kwa-Vonza shopping center (figure 3.1). A

comparison was made between the results from the 3 zones and the two sets of detectors (Tld 200 and the survey meter) that were placed randomly within each zone. The survey meter readings were taken at each point where the TLDs were placed during the placement and the withdrawal of the TLDs and the results presented as an average.

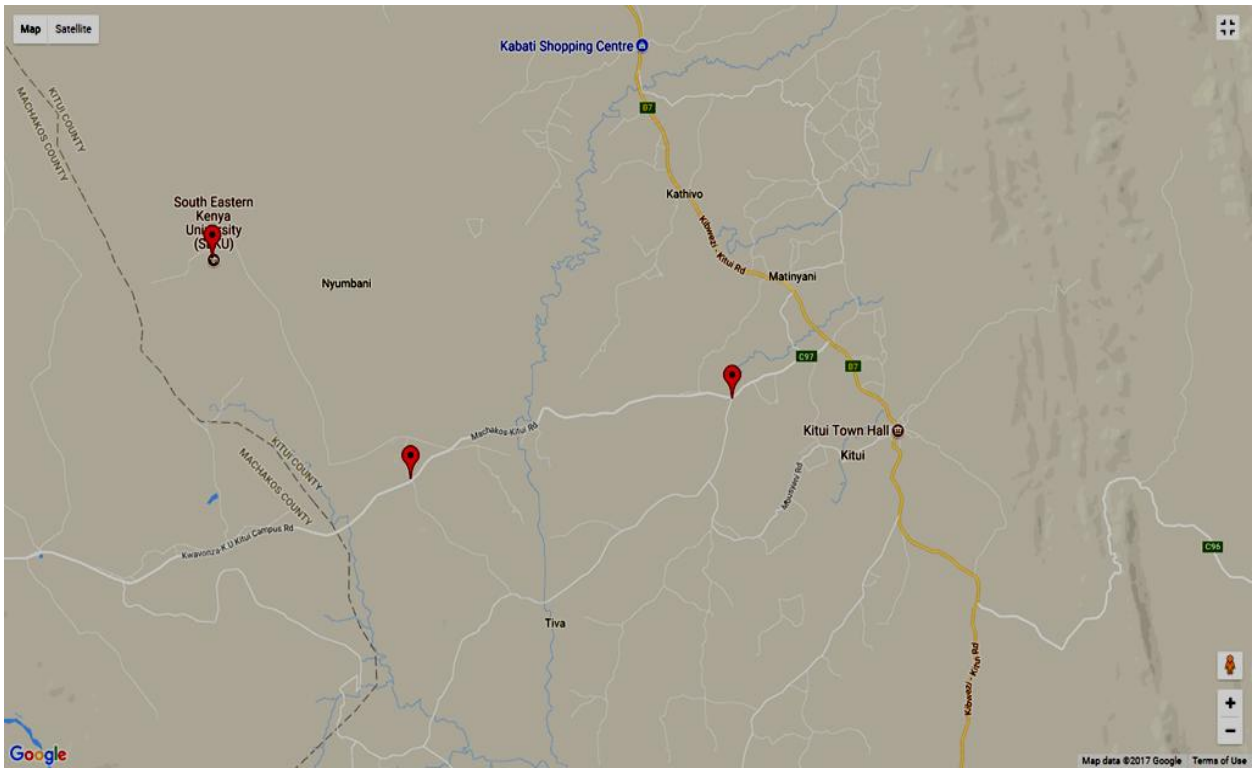

Figure 3.1: Location of the three study zones: SEKU, Kwa-Vonza and Mulutu from left to right respectively.

3.2. The dosimeter

A total of 27 TLD cards obtained from the Kenya Radiation Protection Board and procured from ThermoFisher Scientific Co. ltd, were used in this work. A total of 3 others were used as controls. Examples of the cards are shown in figure 3.2. The cards can hold up to four TLD detectors in form of discs with varying or equal thickness.

During this study, CaF_2: Dy (TLD-200) detectors with dimensions of 1/8" x 1/8" x 0.035" placed inside a TLD card were used. The dosimeters were from two batches of TLD cards consisting of 21 and 7 cards. The first group of 21 TLD cards was of the type TLD-200 containing two Calcium Flouride: Dysporium (CaF_2: Dy) detectors at position 1 and 4 only. The second group of 7 TLD cards consisted of multi-element TLD dosimeters of the type TLDCARD-41C containing two CaF_2: Dy detectors at position 1 and 2 and two LiF: Mg, Ti at positions 3 and 4. In this study, the readings of the two LiF: Mg, Ti detectors were not used because the material is not recommended to be used for environmental dosimetry purposes due to its inability to detect very low environmental doses. The lowest limit of detection for LiF: Mg, Ti is10 μGy compared to that of CaF_2: Dy of 10 pGy.

Figure 3.2: Sample TLD 200 cards and holders

3.3 Annealing and calibration

The annealing of the dosimeters was done on the reader as one batch. During calibration, the exposure was performed with model GC60 Gamma Beam Irradiator with a maximum activity of 2.6 kCi for ^{137}Cs from Hopewell Designs Inc. (fig. 3.3). This irradiator provides a horizontal

radiation beam for calibrating radiation detection instruments and is located at the Kenya Bureau of Standards (KBS) facility.

Figure 3.3.: Model GC60 Gamma Beam Irradiator at KBS

During calibration, the TLD cards were placed 2 meters from the irradiation source and then pinned on a piece of polystyrene whose dimensions were 20 by 20 cm^2 as shown in figure 3.4.

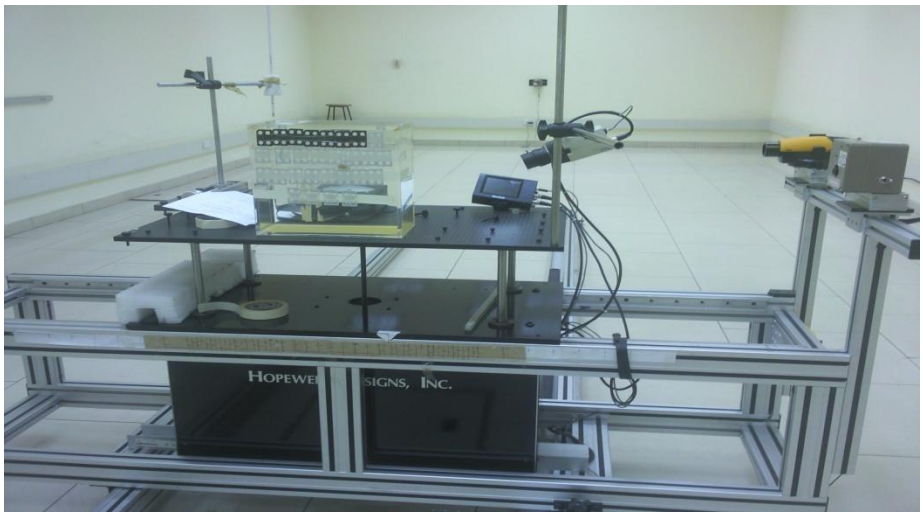

Figure 3.4: Positioning of TLD cards on the polystyrene piece during irradiation

The distance from TLD element to the centre of the irradiation beam was 12.5 cm while the distance between the TLD and the irradiation source was 200 cm. The assumption was that all TLDs were exposed to the same dose despite their position at the polystyrene piece. The TLDs were irradiated at the dose rate of 9.74 mGy hr^{-1} in a ^{137}Cs field for 27 minutes (temperature 23.6 ^{o}C, pressure 840 mbar and humidity 38%). These were the system parameters for the calibrations of TLDs. Background TLDs were not irradiated and their results were used in the determination of the calibration factor during the dose evaluation.

3.4 Storage

Different types of holder design from different manufacturers exist, but the TLD 200 dosimeters used consisted of the card containing four thermoluminescent (TL) elements, and the card holder made of acrylonitrile butadine styrene (ABS) plastic. The holder had front and back pieces that fit together, holding the card inside. The holder or badge were made of thick plastics and contained various filters to modify the amount of radiation reaching the TL elements. The dosimeters were kept away from heat and light during storage by storing them in a dark area.

3.5 Field deployment

The TLDs were deployed in a total of 27 outdoor sites within 3 locations of the study region for a time period of 30 days. A total of 9 dosimeters were assigned to each zone and table 3.1 shows the exact locations for the three zones.

They were installed at least 1 m above the ground outside the dwellings. They were hung on trees, fences and posts as shown in figure 3.5.

Figure 3.5: Placement of TL dosimeters in the field.

Table 3.1 TLD placement locations for SEKU, Kwa-vonza and Mulutu

Dosimeter number	**Location**
SEKU area	
000001	Administration building
000003	Sports field
1000752	Hostel
1000753	Health unit
1000754	Lecture hall
1000755	Maintenance and repairs
1000757	Old gate
1000758	Garden
1000759	Main water tank
Kwa-Vonza area	
000005	KU main gate
000006	Kwa-Vonza primary school
000007	Chief's office
1000760	Garden 1, along R. Mwitasyano
1000761	SEKU hostel
1000762	Lodge, KwaVonza shopping center
1000763	Garden 2, along R. Mwitasyano
1000764	Residence, KwaVonza center
1000765	SEKU main gate
Mulutu area	
000011	Mulutu primary school
000012	Farm next to shopping center

1000766	Garden 1, along R. Tiva
1000767	Residence 1, Mulutu shopping center
1000768	Garden 2, near R. Tiva
1000771	Near Mulutu main water tap
1000772	Residence 2, Near Mulutu center
1000773	Mulutu church
1000774	Garden 3, along R. Tiva

After the exposure period, the exposed TLDs were retrieved and taken to the laboratory for making the reading. The dosimeters were then analyzed using the Harshaw 4500 TLD reader and the absorbed dose calculated. There was no need of transit TLDS as the study region was close. At the time of installing and retrieving the TLDs, the gamma dose rates were taken using the survey meter.

3.6 Readout

The TLD reader that was used in this study was provided by the Kenya Radiation Protection Board and situated in the facility as shown in figure 3.6

Figure 3.6: Tld 4500 reader

CHAPTER 4

RESULTS AND DISCUSSION

In this chapter, the equivalent dose rates are first calculated from the registered field readings. Secondly, the effective doses that were obtained from the TLDs and the survey meter are estimated and finally the comparisons of the values were made.

4.1 Gamma absorbed dose measurements using Thermoluminescent Dosimeters (TLD) and survey meter

The values that were obtained after exposure to ^{137}Cs were first corrected for background by subtracting the average of the values registered by the control TLDs that were not irradiated (appendix A). The readings registered by the field dosimeters in nano coulombs (nC) after 30 days of field exposure are presented in appendix B. Each dosimeter value is an average of the two readings registered by detectors 1 and 2.

The irradiated dose gave the calibration factor that was used in the calculation of the field dose from the field dosimeters values for detectors 1 and 2 contained in each dosimeter holder respectively (appendix C and D). The absorbed dose values from the TLDs and the survey meter were calculated and presented in table 4.1 and 4.2.

Table 4.1: TLD absorbed dose values

Dosimeter No.	Dose(mGy) Detector 1	Dose(mGy) Detector 2	Average Dose (mGy/month)	Absorbed dose (nGy h^{-1})	Dose rates corrected for background (nGy h^{-1})
Control					
1000770	0.095	0.083	0.090	125	
SEKU area					
000001	0.138	0.128	0.134	186	61
000003	0.111	0.105	0.108	150	25
1000752	0.130	0.111	0.121	168	43
1000753	0.110	0.095	0.103	143	18
1000754	0.112	0.082	0.097	135	10
1000755	0.110	0.092	0.101	140	15
1000757	0.162	0.103	0.131	182	57
1000758	0.112	0.104	0.108	150	25
1000759	0.130	0.120	0.125	174	49
Kwa-Vonza area					
000005	0.111	0.111	0.111	154	29
000006	0.121	0.118	0.120	167	42
000007	0.119	0.122	0.121	168	43
1000760	0.101	0.107	0.104	144	19
1000761	0.109	0.085	0.097	135	10
1000762	0.114	0.108	0.111	154	29
1000763	0.131	0.097	0.114	158	33
1000764	0.101	0.085	0.093	129	4
1000765	0.106	0.100	0.103	143	18
Mulutu area					
000011	0.099	0.101	0.100	139	14
000012	0.126	0.116	0.121	168	43
1000766	0.112	0.111	0.112	156	31
1000767	0.112	0.095	0.104	144	19
1000768	0.111	0.112	0.111	154	29
1000771	0.138	0.090	0.114	158	33
1000772	0.105	0.097	0.101	140	15
1000773	0.161	0.109	0.135	188	63
1000774	0.092	0.110	0.101	140	15

Table 4.2: Survey meter dose rate values

Dosimeter number	Dose rate (μSv h^{-1})	Equivalent dose rates (nGy h^{-1})
SEKU area		
000001	0.04	40
000003	0.02	20
1000752	0.04	40
1000753	0.02	20
1000754	0.03	30
1000755	0.04	40
1000757	0.03	30
1000758	0.03	30
1000759	0.04	40
Kwa-Vonza area		
000005	0.01	10
000006	0.02	20
000007	0.02	20
1000760	0.04	40
1000761	0.02	20
1000762	0.02	20
1000763	0.04	40
1000764	0.02	20
1000765	0.08	80
Mulutu area		
000011	0.04	40
000012	0.03	30
1000766	0.05	50
1000767	0.03	30
1000768	0.03	30
1000771	0.01	10
1000772	0.03	30
1000773	0.03	30
1000774	0.04	40

The mean absorbed doses for the entire study area were 30.67nGyh^{-1} for the TLDs and 31.07nGy h^{-1} for the survey meter. The three areas totally registered absorbed doses ranging between 4-63 nGyh^{-1} using TLDs and 10-80 nGy h^{-1} using the survey meter which is the same as 0.03 - 0.39

mSv y^{-1} and 0.06 - 0.49 mSv y^{-1} respectively. The absorbed dose and the annual effective dose equivalent values obtained in the three locations for both methods were calculated and presented in tables 4.3 and 4.4. For the TLDs the highest value was recorded in SEKU (33.67 nGy h^{-1}) followed by Kwa-Vonza (29.22 nGy h^{-1}) and the lowest were from Mulutu area (29.11 nGy h^{-1}) as shown in table 4.3.

Table 4.3: The dose values from the three zones using TLDs

Location		**Absorbed dose rate (nGy h^{-1})**
SEKU area	Range Median Mean Standard Deviation	10-61 25 33.67 20
Kwa -Vonza Area	Range Median Mean Standard Deviation	4-43 29 29.22 13.50
Mulutu Area	Range Median mean Standard Deviation	15-63 15 29.11 16.16
Total	Range Median Mean Standard Deviation	4-63 29 30.67 15.86

Table 4.4. Dose values from the three zones using survey meter

For the survey meter, the highest values were recorded in SEKU (32.22 nGy h^{-1}), followed by Mulutu (31.07 nGy h^{-1}) and the lowest were from Kwa-Vonza area (30 nGy h^{-1}) as shown in figure 4.4

Location		Absorbed dose (nGy h^{-1})
SEKU area	Range Median Mean Standard Deviation	20-40 40 32.22 8.3
Kwa -Vonza Area	Range Median Mean Standard Deviation	10-80 20 30 21.2
Mulutu Area	Range Median mean Standard Deviation	10-50 30 31 11
Total	Range Median Mean Standard Deviation	10-80 30 31.07 13.97

4.2 Comparisons of the TLDs and Survey meter Values

The comparison between the absorbed doses obtained in the three locations for both methods was done and presented in as shown in figure 4.1. The survey meter values were high in all locations with the highest values recorded in SEKU for both dosimeters. The lowest values were recorded in Kwa-Vonza for the survey meter (30 nGy h^{-1}) and Mulutu (29.11 nGy h^{-1}) for the TLDs as shown in figure 4.1.

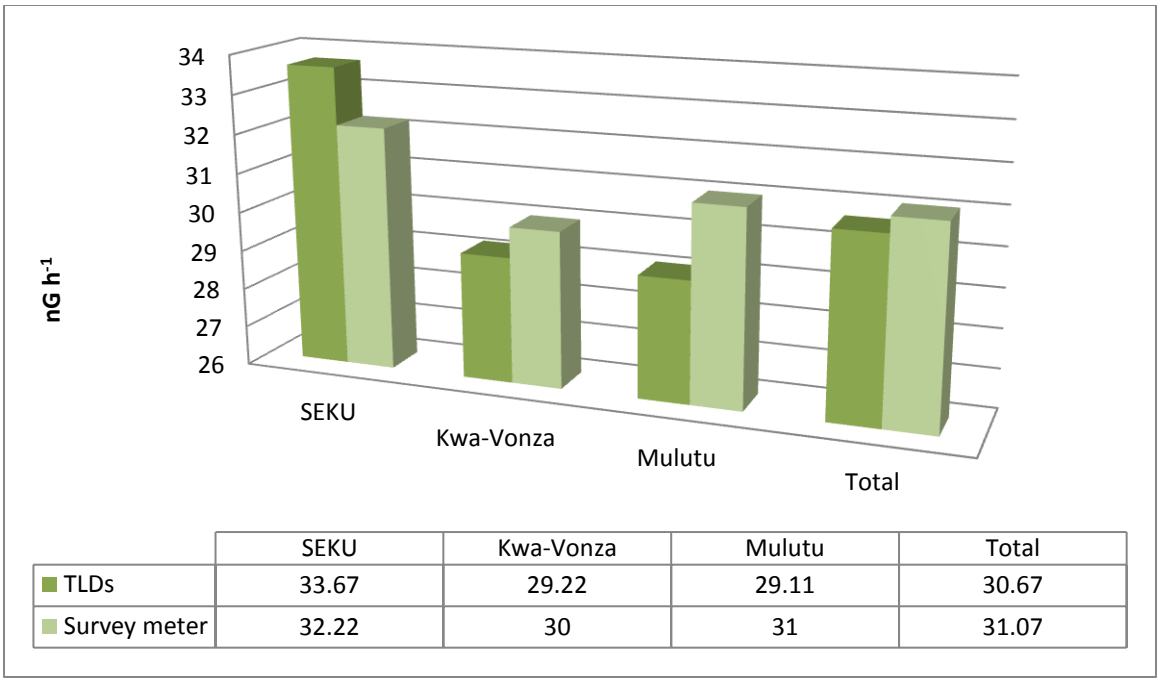

	SEKU	Kwa-Vonza	Mulutu	Total
TLDs	33.67	29.22	29.11	30.67
Survey meter	32.22	30	31	31.07

Figure 4.1 Comparison of the mean annual effective dose from the three zones

The comparison of the dose values recorded in each location was made and presented in figure 4.2. A corresponding regression analysis on these values is done and presented in figure 4.3. It is important to note that the dose registered by the TLDs and the ones recorded by the survey meter did not show a significant difference. This is because both the TLD phosphor that was used (TLD 200) and the Na(Ti) based survey meter are highly sensitive and good for detecting low environmental doses. TLDs give the total dose and the mean dose rate is calculated by dividing with the total field deployment time. For the survey meter, the value at each point represents the average dose rate at that particular time. The statistical uncertainty of the survey meter is therefore small (less than 1%) compared to that of the TLDs which is approximately 5-10%. This is attributed to possible variations between chips, changes in reader conditions and poor statistics as a result of averaging over a small number of chips per dosimeter. This is also a

probable reason for the higher deviations observed with the TLD measurements. However, both detectors can be said to have given a true representation of the dose in the study area.

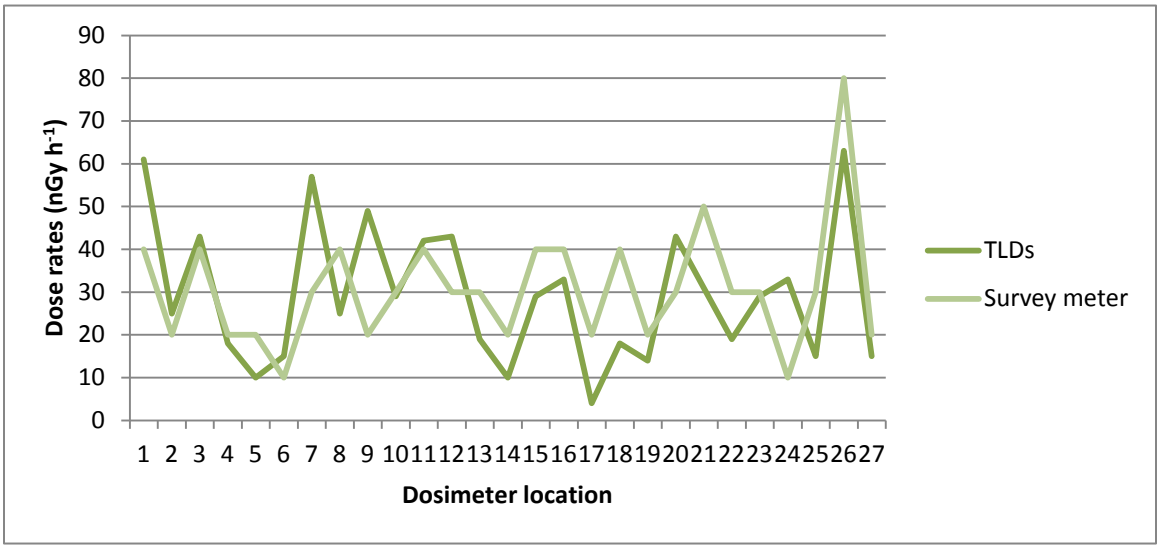

Figure.4.2 A comparison of dose rates registered by TLDs and survey meter in each location

The regression between the variables from the TLDs and survey meter was done and presented in figure 4.3 as shown**.** This shows that the results between the two methods that were used agree. A regression of the values registered by the TLDs and survey meter was positive with r = 0.6.

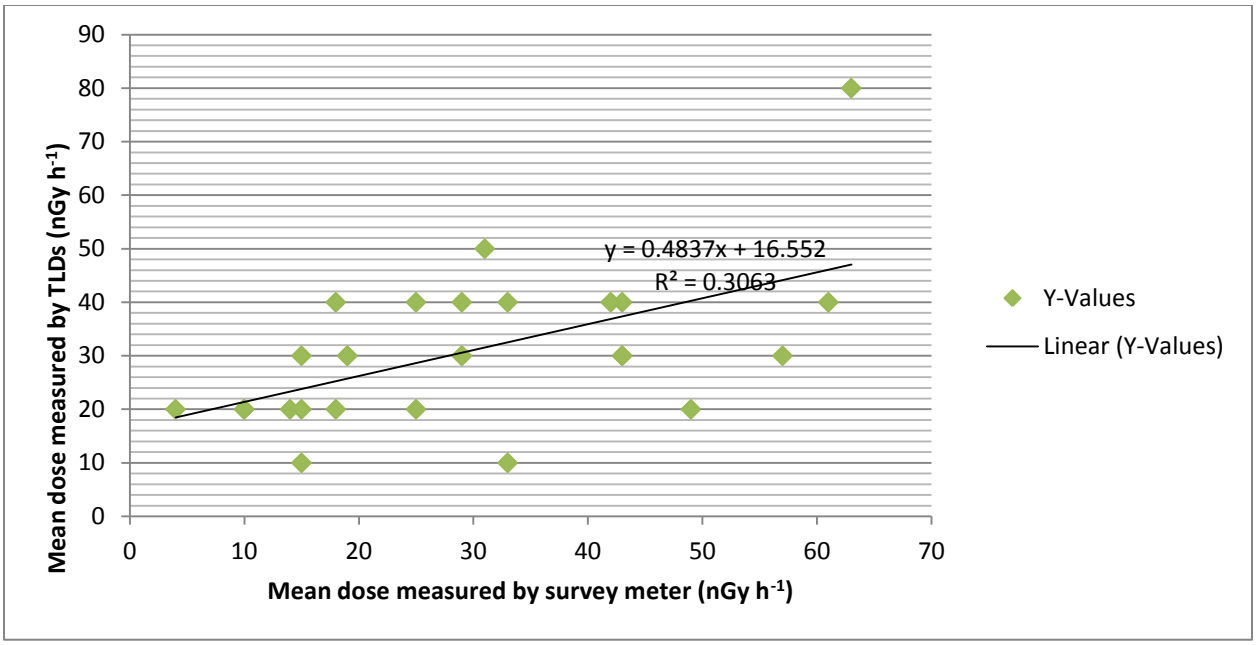

Figure 4.4 Regression of the values obtained by the TLDs and Survey meter

The AEDE (annual effective dose equivalent) was reached at by using the dose conversion factor of 0.7 Sv Gy^{-1} (UNSCEAR, 1993 & UNSCEAR, 2000). Total AEDE (mSv y^{-1}) = D (nGy h^{-1}) x 8760 (h y^{-1}) × 0.7 × 10^{-6}. This gave a result of 0.188 mSv $y^{-1}$for the TLDs and 0.190 mSv y^{-1} for the survey meter.

The change in the amount of dose received with altitude is as a result of cosmic rays. In high background areas, like parts of India, Iran and Brazil, the high doses are as a result of the presence of radioactive components in the soils or bedrock of the area. This was not the case in Kitui as the results shows normal equivalent dose rates that one would expect at that altitude.

In the three areas under study, SEKU area recorded the highest mean dose compared to the other two areas. This can be attributed to the numerous building constructions that were taking place at the university which had huge accumulation of rock and concrete. The difference in the values

obtained from Kwa-Vonza and Mulutu area was minimal. It can be said that the three areas are made of the same bed rock material since they lie within the same altitude and the dose values do not vary significantly.

The results were comparable with others that were obtained in various parts of the world. For instance, Masore et al (2007) obtained an estimated effective dose value of 0.15 mSv y^{-1} in Kwale, Kenya. This is an area that is not far from the study area, Kitui County, which registered a value of 0.19 mSv y^{-1}. The results were also lower than the world average value of 2.4 mSv y^{-1} as well as those obtained in Cameroon (0.48, 0.39 and 0.38 mSv y^{-1}), Nigeria (0.44 and 1.54 mSv y^{-1}), Thailand (0.37 mSv y^{-1}) and Southern India (0.6 mSvy^{-1}).

CHAPTER 5

CONCLUSIONS AND RECOMMENDATIONS

5.1: Conclusion

The amount of dose received in any place increases with altitude and the worldwide average dose rate is 0.03μSv h^{-1}- 0.1mSv h^{-1} at altitudes of between 0 – 2000M above the sea level. The altitude of the study area is between 1170- 1240M and the dose rates that were recorded by both dosimeters of 0.004-0.06 μSv h^{-1} (TLDs) and 0.01-0.08 μSv h^{-1} (survey meter) lie within the world's average range for that altitude. Slight differences are usually brought by the difference in the geological formations of the earth. It can be concluded that Kwa-Vonza area, Kitui County lies within the normal background radiation area of the world. When the linear no threshold model is not applied, the results are much lower than the 1mSv/year threshold which is the maximum allowed occupational dose set by the ICRP.

5.2: Recommendations

Since Kitui County is generally a mineral rich area, it is necessary to carry out continuous radioactivity studies that cover significantly large areas or the whole county. This has to include other radioactivity studies not covered in this study like the radioactivity in soils, radon levels and the determination of sources in the area. Environmental TLD monitoring should also be done over a longer period of time like one year or more to account for the variation during different seasons of the year.

REFFERENCES

Wrixon, A.D. New ICRP recommendations, *Journal of Radiological Protection* 28, no. 2 (6, 2008): 161-168.

Ajayi, O.S., Adesida, G. (2009) Radioactivity in some sachet drinking water samples produced in Nigeria, *Iranian Journal for Radiation Research*, Vol. 7(3), pp.151- 158.

Al Mugren, K.S. (2015) Assessment of Natural Radioactivity Levels and Radiation Dose Rate in Some Soil Samples from Historical Area, Al-Rakkah, Saudi Arabia. *Natural Science*, 7, 238-247.

Antonio E.J, Poston T.M, Rathbone B.A, (2010), Thermoluminescence Dosimeter Use for Environmental Surveillance at the Hanford Site, *Washington Academy of Sciences* 1971-2005.PNL-19207, Pacific Northwest Laboratory, Richland,.

Dyer, C., Lei, F., Hands, A., Truscott, P., (2007) Solar Particle Events in the QinetiQ Atmospheric Radiation Model, IEEE Tran. *Nucl. Sci*., 54, 1071-1075
Forster L., Natural radioactivity and human mitochondrial DNA mutations. Published online October 07, 2002.

Enyinna, P. I. (2016). Radiological risk assessment of cosmic radiation at aviation altitudes (a trip from Houston Intercontinental Airport to Lagos International Airport). *Journal of Medical Physics /Association of Medical Physicists of India*, *41*(3), 205–209. http://doi.org/10.4103/0971-6203.18949.

Elham, B., Masoud, V. M., Asad, B. & Nasrin, F. (2012) Analytical Study Of Radionuclide Concentration And Radon Exhalation Rate In Market Available Building lxiv Materials Of Ramsar, *Journal of Theoretical and Applied Physics*, Vol.6, pp. 7235-7240.

Felix B. Masok, Robert R. Dawam, Emanuel W. Mangset (2015) Assessment of Indoor and Outdoor Background Radiation Levels in Plateau State University Bokkos Jos, Nigeria. *Journal of Environment and Earth Science* ISSN 2224-3216, Vol.5, No.8.

Bochicchio, F., Campos, G., Tommasino, L. Torri, G., (1996) Indoor exposure to gamma radiation in Italy, *IRPA9 Congress Proc.* Vienna, Austria, 2, 190.

Cember, H., Johnson, T. E., (2008) Introduction to health physics

Dodson, R.G. (1953) Geology of the North Kitui Area

Furetta, C. and Weng, P.S. (1998). Operational Thermoluminescence Dosimetry, *World Scientific Publishing*, Singapore. pp. 1-247

Ghiassi-nejad M, Mortazavi SMJ, Niroomand-rad A, Cameron JR,Karam PA. (2002) Very High Background Radiation Areas of Ramsar, Iran: Preliminary Biological Studies. *Health Physics* (in press).

Haug, A. (1972). Theoritical Solid State Physics, Vol II. *Technical University Berlin*. pp. 142-143

Hendry, J.H., Simon, S.L., Wojcik, A., Sohrabi, M., Burkart, W., Cardis, E., (2009) Human exposure to high natural background radiation: what can it teach us about radiation risks? *J RadiolProt*, 29 (2A):A29-42.

ICRP (1991).International Commission on Radiological Protection. 1990 Recommendations of the International Commission on Radiological Protection, *ICRP Publication 60,* Annals of the ICRP 21 (1–3) (Elsevier Science, New York)

Izewska, J. and Rajan, G. (2004): Radiation Dosimeters. *IAEA Publication*, (ISBN 92-0- 107304-6).

Hendry, H.J & Lord, I.B (2002). Radiation Toxicology: Borne Marrow and Leukemia.

Jibiri, N. N, Alausa, S. K, Owofolaju A. E &Adeniran, A.(2011) Terrestrial gamma dose rates and physical-chemical properties of farm soils from ex- tin mining locations in Jos-Plateau, Nigeria, *American Journal of Environmental Science. Technology*, Vol. 5(12), pp. 1039-1049.

Karunakara,N.,Yashodhara, I., Kumara, S., Triptri, R., Menos, S., Kadam, S., and Chougaonkar (2014) Assessment of ambient dose rate around a prspective uranium mining area of south India. *Results in physics*, volume 4, pp. 20-27.

Martin, A. & Harbison, S.A. (1996)An introduction to radiation protection. 3rd ed. New York: *Chapman and Hall*.

Masoomi, J.R, Mohammadi, S., Amin,i M., Ghiassi-Nejad, M. (2006) High background radiation areas of Ramsar in Iran: evaluation of DNA damage by alkaline single cell gel electrophoresis (SCGE). *J Environ Radioact*, 86: 176-86

Matthews, K. & Brennan, P.C. (2008) The application of diagnostic reference levels: General principles and an Irish perceptive. *Radiography*, xx:1-8.

Mortazavi S.M. J. Biological effects of prolonged exposure to high levels of natural radiation in Ramsar, Iran. Proceeding of International Conference on Radiation and its Role in Diagnosis and Treatment, October 2000, Tehran, Iran, in press.

Mortazavi, S.M.J., and Karam, P.A. (2005) Apparent lack of radiation susceptibility among residents of the high background radiation area in Ramsar, Iran: can we relax our standards?

Nair, M.K, Nambi K.S , Amma, N.S ,Gangadharan P. , Jayalekshmi P., Jayadevan S. , Cherian V. , Reghuram K.N. (1999) Population study in the high natural background radiation area in Kerala, India. *Radiat Res*, 152(6 Suppl): S145-8.

Najat, K. and Mohamed, S. (2013) Natural Radioactivity in Soil and Water from Likuyu Village in the Neighborhood of Mkuju Uranium Deposit, *International Journal of Analytical Chemistry*, vol. 2013, Article ID 50185, doi:10.1155/2013/501856

Oktay, B., Sule, K.& Mahmut, D.(2011) Assessments of natural radioactivity and radiological hazards in construction materials used in Elazig, Turkey, *Radiation Measurements*, Vol. 46, pp. 153-158

Ranogajec-Komor, M. (2003). Thermoluminescence dosimetry application in environmental monitoring. *Radiation Safety Management* Vol.2, 1: 2-16.

McKeever, S.W., Moscovich, M. and Townsend, P.D. (1995). Thermoluminescence dosimetry materials: properties and uses .*Nuclear Technology Publishing*, Ashford.

Sroor, A, El-Bahi, S. M, Ahmed, F. & Abdel-Haleem, A. S (2001) Natural radioactivity and radon exhalation rate of soil in southern Egypt, *Applied Radiation and Isotopes*, Vol. 55, pp. 873–879.

Stochiou, A. I., Scarlat, F., Georgescu, I.I. and Alexiu, F. (2004). Method to Manufacture Thermoluminescent Detector Chips using LiF Crystal. *Journal of Optoelectronics and Advanced Materials* Vol.6, No.4,: 1357-1363.

Thompson, R.E. (2011) Epidemiological Evidence for Possible Radiation Hormesis from Radon Exposure: A Case-Control Study Conducted in Worcester, MA. *Dose Response*, 9: 59-75.

Todsadol, S. (2012). An Evaluation of the Level of Naturally Occurring Radioactive Materials in Soil samples along the Chao Phraya River Basin, PHD Thesis, University of Surrey.

Trapp, J.V. & Kron, T. (eds) (2008). An introduction to radiation protection in medicine. New York: Taylor & Francis.

UNSCEAR- United Nations Scientific Committee on the Effects of Atomic Radiation (1993) Sources, Effects and Risks of Ionizing Radiation. United Nations, New York

United Nations Scientific Committee on the Effects of Atomic Radiation (2000) Sources, Effects and Risks of Ionizing Radiation, International Atomic Energy Agency, Vol. 1.

United Nations Scientific Committee on the Effects of Atomic Radiation, Sources and effects of Ionizing Radiation. New York: UNSCEAR, 2008. Update 2012

Zakeri F, Rajabpour MR, Haeri SA, Kanda R, Hayata I, Nakamura S, (2011) Chromosome aberrations in peripheral blood lymphocytes of individuals living in high background radiation areas of Ramsar, Iran. *RadiatEnvi-ronBiophys*, 50: 571-8. 21.

Zha Y.R, Tao Z.F, Wei L.X, (1996) Epidemiological survey in a high background radiation area in Yangjiang. *Chung Hua Liu Hsing Ping HsuehTsaChih*, 17(6): 328-332.

APPENDICES

Appendix A: Control values

Laboratory

Dosimeter number	Detector 1(nC)	Detector 2(nC)
000008	739.37	167.28
1000769	223.84	453.57

Field

Dosimeter number	Environmental reading (nC)		Calibration reading (nC)		Average dose rate (nGy h^{-1})
	Detector 1	**Detector 2**	**Detector 1**	**Detector 2**	
1000770	**68.627**	**65.465**	**3153.7**	**3469.2**	**125**

Appendix B: Dosimeter reading after exposure to ^{137}Cs

Dosimeter No.	**Dosimeter readings**		**Dosimeter readings corrected for background**	
	Detector 1(nC)	Detector 2 (nC)	Detector1(nC)	Detector2(nC)
000001	4834.4	4783.9	4438.4	4387.9
000003	5192.7	4690.5	4796.7	4294.5
000005	5123	4639.5	4727	4243.5
000006	4883.3	4184.3	4487.3	3788.3
000007	5124.7	4619.7	4728.7	4223.7
000011	5166.9	4287.2	4770.9	3891.2
000012	4754.2	4391.2	4358.2	3995.2
1000752	3790.3	3998.3	3394.3	3602.3
1000753	3998	4121	3602	3725
1000754	4658.4	4097.8	4262.4	3701.8
1000755	3899.8	4176	3503.8	3778
1000757	4003.8	4245.7	3607.8	3849.7
1000758	4048.9	3846.7	3652.9	3450.7
1000759	4035.8	4434.7	3639.8	4038.7
1000760	4119.8	5114.6	3723.8	4718.6
1000761	3911.6	3968.9	3515.6	3572.9
1000762	3852.5	4207.4	3456.5	3811.4
1000763	4271	3958.3	3875	3562.3
1000764	3732.1	4011.7	3336.1	3615.7
1000765	3997.8	4130.8	3601.8	3734.8
1000766	3557.3	4237.8	3161.3	3841.8
1000767	3721.1	4213.7	3325.1	3817.7
1000768	3911.9	4013.8	3515.9	3617.8
1000770	3153.7	3469.2	2757.7	3073.2
1000771	3863.5	3736.4	3467.5	3340.4
1000772	4233.2	4364.9	3837.2	3968.9
1000773	3578.4	3973.6	3182.4	3577.6
1000774	3687.7	4935.6	3291.7	4339.6

Appendix C: Dosimeter readings after field exposure

Dosimeter No.	Detector 1(nC)	Detector2(nC)
000001	152.79	139.67
000003	131.57	112.18
000005	129.29	117.9
000006	135.02	112.88
000007	139.55	129
000011	116.53	99.071
000012	136.58	116.33
1000752	112.1	101.18
1000753	97.14	89.052
1000754	118.58	76.847
1000755	98.131	87.312
1000757	147.9	99.703
1000758	103.72	90.885
1000759	119.64	121.11
1000760	94.916	124.38
1000761	97.218	77.098
1000762	100.57	103.71
1000763	127.2	87.689
1000764	85.614	77.796
1000765	96.917	94.189
1000766	91.262	107.73
1000767	94.9	91.33
1000768	99.391	103
1000770	68.627	65.465
1000771	121.77	77.047
1000772	101.53	96.554
1000773	131.59	99.012
1000774	77.489	124.06

AppendixD: Absorbed dose values for Detector 1 after one month field exposure

Dosimeter No.	Position1 Environmental dose (nC)	Position1 Calibration dose (nC)	Dose (mGy)
000001	152.79	4438.4	0.138
000003	131.57	4796.7	0.111
000005	129.29	4727	0.111
000006	135.02	4487.3	0.121
000007	139.55	4728.7	0.119
000011	116.53	4770.9	0.099
000012	136.58	4358.2	0.126
1000752	112.1	3394.3	0.130
1000753	97.14	3602	0.110
1000754	118.58	4262.4	0.112
1000755	98.131	3503.8	0.110
1000757	147.9	3607.8	0.162
1000758	103.72	3652.9	0.112
1000759	119.64	3639.8	0.130
1000760	94.916	3723.8	0.101
1000761	97.218	3515.6	0.109
1000762	100.57	3456.5	0.114
1000763	127.2	3875	0.131
1000764	85.614	3336.1	0.101
1000765	96.917	3601.8	0.106
1000766	91.262	3161.3	0.112
1000767	94.9	3325.1	0.112
1000768	99.391	3515.9	0.111
1000770	68.627	2757.7	0.095
1000771	121.77	3467.5	0.138
1000772	101.53	3837.2	0.105
1000773	131.59	3182.4	0.161
1000774	77.489	3291.7	0.092

Appendix E: Absorbed dose values for detector 2 after one month field exposure

Dosimeter No.	Position2 Environmental reading(nC)	Position2Calibration reading(nC)	Dose(mGy)
000001	139.67	4783.9	0.128
000003	112.18	4690.5	0.105
000005	117.9	4639.5	0.111
000006	112.88	4184.3	0.118
000007	129	4619.7	0.122
000011	99.071	4287.2	0.101
000012	116.33	4391.2	0.116
1000752	101.18	3998.3	0.111
1000753	89.052	4121	0.095
1000754	76.847	4097.8	0.082
1000755	87.312	4176	0.092
1000757	99.703	4245.7	0.103
1000758	90.885	3846.7	0.104
1000759	121.11	4434.7	0.120
1000760	124.38	5114.6	0.107
1000761	77.098	3968.9	0.085
1000762	103.71	4207.4	0.108
1000763	87.689	3958.3	0.097
1000764	77.796	4011.7	0.085
1000765	94.189	4130.8	0.100
1000766	107.73	4237.8	0.111
1000767	91.33	4213.7	0.095
1000768	103	4013.8	0.112
1000770	65.465	3469.2	0.083
1000771	77.047	3736.4	0.090
1000772	96.554	4364.9	0.097
1000773	99.012	3973.6	0.109
1000774	124.06	4935.6	0.110